JCTC Journal of Chemical Theory and Computation

Article

pubs.acs.org/JCTC

What Exactly Is the Light Emitter of a Firefly?

Yuan-Yuan Cheng and Ya-Jun Liu*

Key Laboratory of Theoretical and Computational Photochemistry, Ministry of Education, College of Chemistry, Beijing Normal University, Beijing 100875, China

Supporting Information

ABSTRACT: Firefly bioluminescence attracts people by its glaring beauty and fascinating applications, but what is the light emitter of a firefly? The answer to this question has been explored since before the 1960s. The unanimously accepted answer is that excited-state oxyluciferin is the light emitter. The complexity of this question arises from the existence of six chemical forms (keto, enol, keto-1, enol-1, enol-1′, and enol-2) of oxyluciferin. After decades of experimental and theoretical efforts, a consistent conclusion was almost reached in 2011: excited-state keto-1 is the only light emitter in fireflies. However, the debate is raised again by the latest in vitro experimental results. This study will solve this contradiction via hybrid quantum mechanics and molecular mechanics (QM/MM) calculations combined with molecular dynamics (MD). The calculations were performed in the real protein for the six chemical forms of oxyluciferin and their corresponding analogues employed in the latest experiments. By considering the real environment, the pH value, and a possible equilibrium of the chemical forms of oxyluciferin in vivo, the calculated results indicate that the main emitter is still the excited-state keto-1 form.

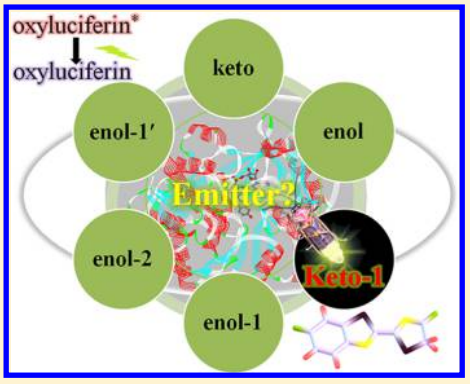

INTRODUCTION

Bioluminescence, a phenomenon of emitting light by a living organism, is widespread in nature and makes nature more colorful. The firefly is found all over the world and is the most common living bioluminescent thing. Because of its high quantum yield[1] and high signal-to-noise ratio, firefly bioluminescence is found in extensive applications, mainly as an analytical tool.[2−4] The generally accepted process of firefly bioluminescence is that luciferase catalyzes the oxidation of luciferin in the presence of ATP, Mg^{2+}, and O_2 to form a dioxetanone. Light is emitted by the light emitter after it is produced via the thermolysis of the dioxetanone.[5,6] The complicated process for generating the light emitter[7−9] has been extensively studied; therefore, we will only focus on the identification of the light emitter.

There is no doubt that the light emitter of the firefly is excited-state oxyluciferin based on previous experimental[10−12] and theoretical[13−15] studies. The problem is that oxyluciferin has six chemical forms (keto, enol, keto-1, enol-1, enol-1′, and enol-2), as shown in Figure 1. What are the difficulties in identifying the light emitter? First, it is hard to isolate each chemical form of oxyluciferin in the lab for an investigation of the corresponding fluorescence spectrum. Several forms of oxyluciferin are liable to coexist in solution, and the pure form of each has not been obtained until now.[16] Recently, some groups have used analogues of oxyluciferins[11,17] to constrain the ionization of both hydroxyl groups and the keto−enol tautomerization of the thiazole moiety and to obtain the absorption and emission spectra of these oxyluciferin analogues. The spectra of these analogues reflects the luminescence properties of the corresponding oxyluciferin. However, the spectra were measured in vitro and could be very different from those measured in vivo because the polarity, pH, and H-bonding networks of the environment greatly affect the spectral properties.[11,17−20] In addition, the multicolor phenomenon makes the identification of the light emitter trickier. The structure of luciferin is the same for various luciferases;[21,22] however, the emitted light naturally ranges from green (530 nm) to red (635 nm).[6,23] There are three interpretations to explain this phenomenon: (1) The light emitter has more than one chemical form. As early as 1971, White et al.[24] proposed the existence of keto−enol equilibrium. The hypothesis that the light emitter is of different twisted structures was also put forward[25] but was ruled out by theoretical studies.[26−28] (2) There is only one chemical form of the light emitter, which is keto-1, and microenvironmental effects allow for the emission of the different colors of light. Branchini et al.[29] proposed that the luciferase controls the resonance structure of keto-1, which modulates the color of the emitted light. Later, the resonance structure was identified in a theoretical study.[15] In addition, the emitter should emit yellow-green light in a closed form and red light in an open form of luciferase.[30] Subsequently, both experiments[10,18,19] and theoretical computations[14,15] suggested that the color is modulated not by the rigidity of the active site but rather by the polarity near the phenolate oxygen of keto-1. (3) The joint effect of various chemical forms and different microenvironments modulate the color. More recently, Ran et al.[31] found that the emission of colors can be obtained from various oxyluciferin forms and is influenced by luciferase.

Received: July 9, 2015
Published: October 9, 2015

DOI: 10.1021/acs.jctc.5b00659
J. Chem. Theory Comput. 2015, 11, 5360−5370

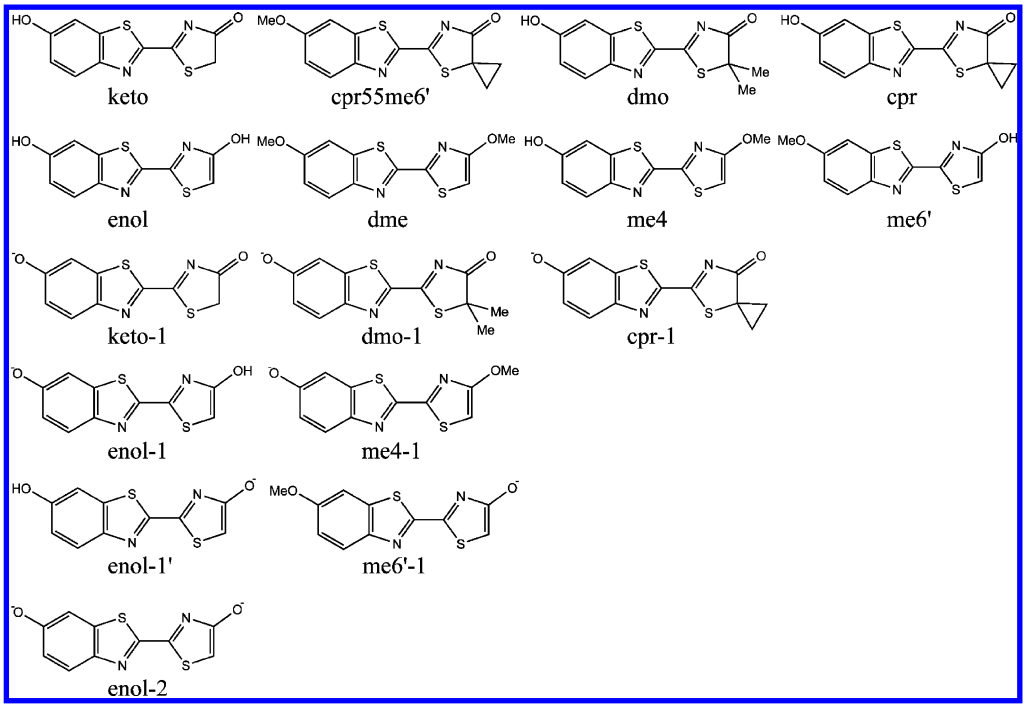

Figure 1. Molecular structures of all possible chemical forms of firefly oxyluciferin and their corresponding analogues.

For the chemical form of the firefly light emitter to be identified, many experimental[10−12,17,19,20,29,32] and theoretical[13,28,33−39] studies have been performed. Before 2011, some theoretical investigations, such as quantum mechanics/molecular mechanics (QM/MM) calculations,[14] supported the conclusion that keto-1 is the emitter in luciferase. This conclusion is consistent with previous experimental results.[12,29] However, Naumov et al.[19] reported the crystal structure of oxyluciferin in the enol form for the first time and inferred that enol-1 is the most probable emitter. Subsequently, they studied the keto−enol−enolate and phenol−phenolate equilibria of oxyluciferin using spectral research of analogues in various solutions and found that enol-1′ emits yellow light and that red emission may come from enol-2 or keto-1.[20] In 2011, in the face of these disputes, Chen et al.[13] systematically calculated all of the possible chemical forms using a multireference method and concluded that keto-1 is the direct product of the excited-state decomposition of firefly dioxetanone in vivo and the only light emitter of firefly in natural bioluminescence. Moreover, a study of the effect of pH on the different chemical equilibria of oxyluciferin by Pinto da Silva et al.[38] and QM/MM and molecular dynamics (MD) studies by Song et al.[37] support the same conclusion. Recently, a different conclusion was put forward by Pinto da Silva et al.,[39] who proposed that the enolate ion is the emitter based on a theoretical approach in an enzymatic-like microenvironment. Ghose et al.[11] researched the emission properties of oxyluciferin and analogues in a buffered aqueous solution and implied that enol-1′ is the most likely emitter. Both studies have a common problem: They were not carried out in vivo. For bioluminescence, it is necessary to consider the question in luciferase, which was also realized in the most recent study.[31] In addition, Ugarova et al.[40] put forward an idea of a triple equilibrium, where the emitter simultaneously exists in more than one form in equilibrium. The superposition of emission from each form generates the yellow-green light.

To identify the emitter, we have systemically investigated the emission properties of the six chemical forms of oxyluciferin and their 10 analogues[11,17] in the gas phase, in toluene, in water, and in the protein environment using molecular simulations based on QM, QM/MM, and MD calculations at the same level. For reducing the CPU time, the calculations in the gas phase and in different solutions provide good initial structures and starting information for the calculations performed in the real protein environment. Although we have performed calculations on the six chemical forms before,[13] new experimental data[11] have recently been obtained; therefore, a more systematic calculation including the various analogues is needed at the same computational level. The analogues and the six chemical forms of oxyluciferin have the following relationship: dmo, cpr, and cpr55me6′ corresponding to keto; me4, me6′, and dme corresponding to enol; dmo-1 and cpr-1 corresponding to keto-1; me4-1 corresponding to enol-1; and me6′-1 corresponding to enol-1′ (for the abbreviations and related structures, see Figure 1). This paper is organized such that the computational methods are introduced prior to the Results and Discussion section. In the Results and Discussion section, the information provided below for the six chemical forms and their 10 analogues is presented and discussed in the following order: first, the optimized structures of the ground (S_0) and first singlet excited (S_1) states; second, the absorption and fluorescence spectra; third, the influence of pH on the spectra in aqueous solution; and fourth, the possible triple equilibrium in protein. Afterwards, our conclusions are presented.

COMPUTATIONAL METHODS

QM Calculations. All QM calculations were performed using density functional theory (DFT)[41,42] and time-dependent DFT (TD DFT).[43,44] The Coulomb-attenuated hybrid exchange-correlation functional (CAM-B3LYP)[45] was employed, which combines the features of the B3LYP[46,47] with long-range corrections using Hartree−Fock (HF) exchange

DOI: 10.1021/acs.jctc.5b00659
J. Chem. Theory Comput. 2015, 11, 5360−5370

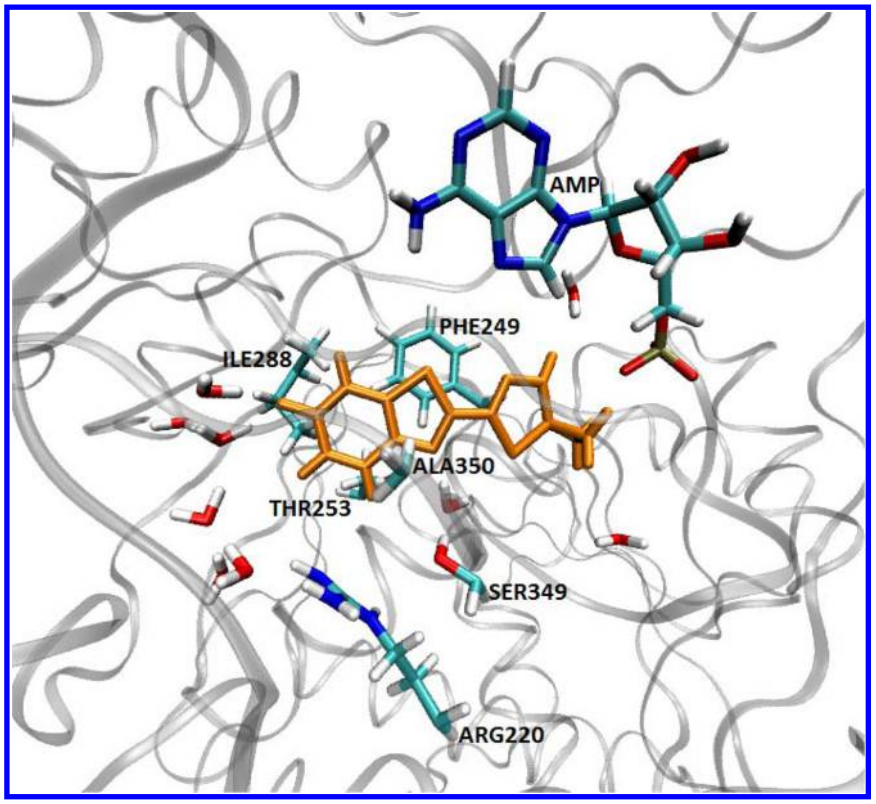

Figure 2. QM/MM computational model. The QM/MM optimization was performed with cpr-1 (in orange) in its S_1 state in the QM region. AMP and the six side chains (Arg220, Phe249, Thr253, Ile288, Ser349, and Ala350) and selected water molecules within 5 Å of cpr-1 (O in red, C in cyan, N in blue, H in white, and P in tan) were allowed to relax. All other atoms were frozen. Oxyluciferin and other oxyluciferin analogues have similarly defined QM and MM regions. The gray ribbon in the background represents the protein environment.

because it can improve the description of charge transfer (CT) excited states and has been verified in previous works.[48,49] The geometries of the S_0 states of oxyluciferin and oxyluciferin analogues were optimized at the CAM-B3LYP/6-31G** level in water. On the basis of the optimized S_0 geometries, the absorption maximum (λ_{max}) and oscillator strength (f) were predicted at the TD CAM-B3LYP/6-31G** level. The geometries of the optimized S_1 states of oxyluciferin and oxyluciferin analogues were also obtained at the level of TD CAM-B3LYP/6-31G** in the gas phase, in toluene, and in water. On the basis of the optimized S_1 geometries, the fluorescence wavelength (λ_F) and f were predicted at the level of TD CAM-B3LYP/6-31G**. For the nonpolar solvent toluene, the polarizable continuum model (PCM)[50,51] was employed in the self-consistent reaction field calculations, whereas for the polar solvent water, the conductor-like polarized continuum model (C-PCM)[52] was used. The above calculations were performed using the Gaussian09 program package.[53]

QM/MM Calculations. The geometry optimization for the S_1 states and prediction of λ_F and f for oxyluciferin and oxyluciferin analogues were calculated in a protein environment. The calculations were performed using the QM/MM coupling scheme implemented in a local modified version of the Gaussian and Tinker[54] packages. The electrostatic interaction is a vital coupling between the QM and MM subsystems, considering that the simulated two different local electrostatic fields of enzymatic-like microenvironments induce different emission energies of oxyluciferin.[55] The electrostatic potential fitted (ESPF) method[56] was used to achieve the electrostatic coupling. The microiterations technique was used to converge the MM subsystem geometry at every QM optimization step. In all of the computational models, the oxyluciferin and oxyluciferin analogues comprised the QM region, whereas the remaining atoms were included in the MM region. During the geometry optimizations, the AMP and six side chains (Arg220, Phe249, Thr253, Ile288, Ser349, and Ala350) and water molecules within 5 Å of oxyluciferin (oxyluciferin analogues) were allowed to relax in the MM subsystem, whereas all other water and protein atoms in the MM region were kept frozen (see Figure 2 and the details in the Supporting Information (SI)). It does not improve the calculated results when the relaxed water molecules are expanded to 10 Å around oxyluciferin (oxyluciferin analogues) (see details in Table S9). The geometries of oxyluciferin and oxyluciferin analogues were optimized in the S_1 state with the TD CAM-B3LYP functional because our study focused on the calculation of λ_F values, i.e., the energy of the vertical emission transition from the S_1 state minimum to the S_0 state. Because no analytical second derivatives are currently available in the TD DFT method and because a numerical procedure would be too expensive, the exact nature of the optimized QM/MM stationary points has not been verified. The 6-31G** basis set was employed for the QM region, and the AMBER Parm99SB force field,[57] as described below, was used for the MM region. The vertical emission transition energies have been computed at the TD CAM-B3LYP/6-31G**/MM theoretical level.

Force Field Parameters for AMP and the S_1 States of Oxyluciferin and Oxyluciferin Analogues. The AMBER Parm99SB force field was used to model the residues of firefly luciferase. We assigned the atom types of oxyluciferin and oxyluciferin analogues based on the standard AMBER atom

DOI: 10.1021/acs.jctc.5b00659
J. Chem. Theory Comput. 2015, 11, 5360−5370

type. We used the equilibrium bond lengths, bond angles, dihedral angles, force constants, and van der Waals parameters for atom types similar to those defined in the AMBER Parm99SB force field. The restricted electrostatic potential (RESP) charges were determined by the RESP fitting protocol implemented in the ANTECHAMBER module of the AMBER9 package[58] after making calculations of ESP at the HF/6-31G** level. The AMP parameters developed by Navizet et al.[14] were used.

Computational Models. The X-ray crystallographic structure of firefly luciferase (PDB ID: 2D1S)[30] was used as the starting structure. In fireflies, the 5′-*O*-[*N*-(dehydroluciferyl-)-sulfamoyl] adenosine (DLSA) is bound in the cavity. For instance, for cpr-1, the DLSA was replaced by cpr-1 + AMP (Figure 3). To study the S_1 state of cpr-1 in firefly luciferase, we

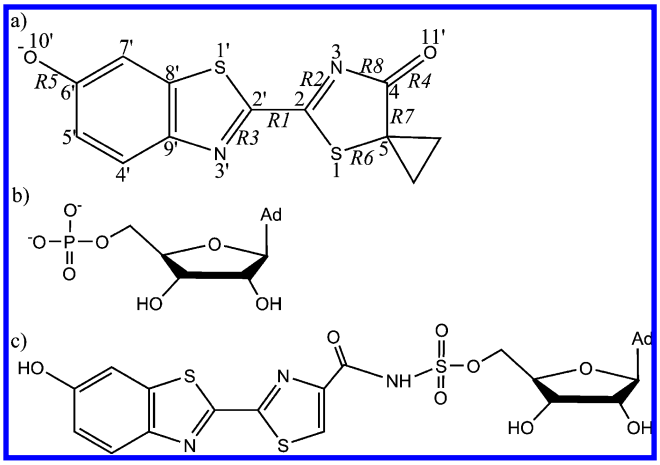

Figure 3. Structures of (a) cpr-1, (b) AMP, and (c) DLSA and labels.

first performed a 1 ns MD simulation starting from the 2D1S structure. The minimum-energy structure for cpr-1, observed between 150 and 250 ps of the trajectories, was extracted (Figure S1). After the MM minimization starting from the MD minimum-energy structure, a QM/MM optimization of the S_1 state of cpr-1 was performed. On the basis of the MD minimum-energy structure of cpr-1, the MM minimization and QM/MM optimization for the S_1 states of oxyluciferin and other oxyluciferin analogues were also performed. More details can be found in the SI.

RESULTS AND DISCUSSION

Structural Analysis of the Six Chemical Forms of Oxyluciferin and Their 10 Analogues. The geometries of the S_0 states of the six chemical forms of oxyluciferin and their 10 analogues were optimized at the level of CAM-B3LYP/6-31G** in water. The geometries of the S_1 states of the six chemical forms of oxyluciferin and the 10 analogues were optimized at the level of TD CAM-B3LYP/6-31G** in the gas phase, in solution (i.e., toluene and water), and in the protein environment at the level of TD CAM-B3LYP/6-31G**/MM. The optimized main bond lengths of the S_0 and S_1 states of the six chemical forms of oxyluciferin and their 10 analogues in water are reported in Table 1. The optimized main parameters in the gas phase, in toluene, and in the protein are listed in Tables S1−S3.

The optimized key bond lengths of the S_0 state of enol and dmo in water are similar to those in the crystal,[18,19] which indicates that the theoretical approach is reliable. The predominant variations between the geometries of the S_0 and S_1 states for all of the compounds is in the -N═C−C═N- unit, where the *R1* bond is shortened by 0.013−0.077 Å, whereas the *R2* and *R3* bonds are elongated by 0.014−0.068 Å (for the description of the labels, see Figure 3; for the detailed data, see Table 1) from the S_0 state geometry to the corresponding S_1 state.

By comparing the key bond lengths of each chemical form and their corresponding analogues, we can see that the O11′ and O10′-methyl substituents hardly affect the bond length. In addition, two C5-methyl substituents make *R6* and *R7* slightly longer, whereas the C5-spirocyclopropyl substituent results in slightly shorter bonds. By comparing the corresponding geometrical parameters in the neutral molecules and ions (Table 1), we can see that between enol (me6′) and enol-1′ (me6′-1), for ions, *R4* is shorter, whereas *R7* and *R8* are longer in the S_0 state. In the S_1 state, *R1*, *R5*, *R7*, and *R8* are longer and *R2*, *R3*, and *R4* are shorter. When comparing enol (me4) and enol-1 (me4-1), for ions, *R1* and *R5* are shorter in the S_0 state, *R1*, *R4*, and *R6* are longer, and *R5* and *R7* are shorter in the S_1 state. For keto (dmo and cpr) and keto-1 (dmo-1 and cpr-1), for ions, *R1*, *R5* and *R8* are shorter, and *R2* and *R3* are longer in the S_0 state, whereas *R3* and *R5* are shorter in the S_1 state. Among these bonds, the *R1* bond in the S_0 state for keto-1 (dmo-1 and cpr-1) is similar to a C═C bond length (1.34 Å). This finding indicates that keto-1 (dmo-1 and cpr-1) has resonance structures in the S_0 state (Scheme S1). Compared with the geometrical parameters of enol-1, the geometrical parameters of enol-2 are more similar to those of enol-1′ with the exception that *R5* is shorter in the S_0 state and that *R1* and *R5* are shorter and *R2* and *R3* are longer in the S_1 state.

How does the environment affect the geometries of the six chemical forms of oxyluciferin and their 10 analogues? Below, we only compare the important bond lengths of these compounds in the S_1 state in the gas phase, in toluene, in water, and in the protein (for details, see Table 1 and Tables S1−S3). First, we compare the bond lengths in the gas phase and in a toluene solution. In the gas phase, for enol-1 (me4-1), *R1* is longer and *R3* is shorter; for enol-1′ (me6′-1), *R1* and *R6* are longer and *R7* is shorter; for the keto analogues, the geometrical parameters of both cpr and cpr55me6′ are much different from those of keto. The composition of the major transition configuration is obviously lower for cpr and cpr55me6′ (Table S5). Second, we compare the bond lengths in toluene and in water. For all ions in water, *R1* is shorter and *R2* and *R3* are longer. Moreover, for enol-1′ (me6′-1), *R6* and *R8* are shorter and *R7* is longer; for keto (cpr55me6′, dmo and cpr), *R2* is slightly longer and *R5* is slightly shorter. The above bonds are significant to the electronic transition leading to the corresponding S_1 state for these compounds (Figures S4−S7). The structural variation among the different types of compounds is related to the variation in the corresponding fluorescence. Third, we compare the bond lengths in toluene and in a protein environment. The bond lengths of cpr55me6′ and dmo-1 in the protein are similar to those computed in toluene because there are no strong hydrogen-bonding interactions around them. For the other compounds, the bond length variation between toluene and the protein environment is primarily found for *R4*, *R5*, *R6*, and *R7*, which is related to the interaction with a protein environment surrounding O10′, O11′, and C5 in these compounds (Figures S10−S15). In addition, the S_1-state geometries of all oxyluciferins and their analogues are planar in the gas phase, in

DOI: 10.1021/acs.jctc.5b00659
J. Chem. Theory Comput. 2015, 11, 5360−5370

Table 1. Predicted Key Bond Lengths (Å) of the S_0 (First Line) and S_1 (Second Line) State of the Six Chemical Forms of Oxyluciferin and Their 10 Analogues by CAM-B3LYP/6-31G** and TD CAM-B3LYP/6-31G** Optimized in Water

	R1	R2	R3	R4	R5	R6	R7	R8
keto	1.456	1.288	1.293	1.208	1.353	1.809	1.531	1.404
	1.400	1.327	1.361	1.225	1.324	1.811	1.541	1.365
cpr55me6′	1.456	1.289	1.292	1.213	1.352	1.791	1.501	1.403
	1.397	1.330	1.360	1.229	1.320	1.788	1.515	1.364
dmo	1.456	1.290	1.293	1.210	1.353	1.835	1.542	1.400
	1.400	1.330	1.361	1.227	1.324	1.836	1.551	1.362
cpr	1.456	1.289	1.293	1.213	1.353	1.791	1.500	1.403
	1.397	1.330	1.360	1.229	1.325	1.787	1.515	1.364
enol	1.453	1.304	1.291	1.348	1.357	1.724	1.366	1.363
	1.377	1.346	1.356	1.338	1.345	1.712	1.399	1.335
dme	1.454	1.302	1.290	1.343	1.356	1.725	1.368	1.366
	1.377	1.344	1.357	1.334	1.341	1.713	1.399	1.339
me4	1.454	1.302	1.291	1.343	1.357	1.726	1.367	1.366
	1.377	1.344	1.356	1.333	1.345	1.712	1.400	1.339
me6′	1.454	1.304	1.290	1.348	1.356	1.724	1.366	1.363
	1.377	1.346	1.356	1.339	1.342	1.712	1.398	1.336
keto-1	1.421	1.303	1.313	1.215	1.253	1.808	1.535	1.385
	1.407	1.329	1.344	1.228	1.249	1.811	1.541	1.362
dmo-1	1.421	1.305	1.313	1.217	1.254	1.832	1.545	1.381
	1.408	1.331	1.343	1.231	1.249	1.836	1.551	1.359
cpr-1	1.423	1.304	1.312	1.219	1.254	1.791	1.507	1.385
	1.406	1.331	1.344	1.232	1.249	1.793	1.515	1.361
enol-1	1.444	1.306	1.297	1.351	1.262	1.731	1.363	1.365
	1.390	1.348	1.352	1.355	1.253	1.736	1.379	1.341
me4−1	1.444	1.305	1.297	1.346	1.263	1.733	1.364	1.368
	1.391	1.346	1.352	1.351	1.253	1.737	1.380	1.344
enol-1′	1.452	1.297	1.292	1.258	1.360	1.728	1.406	1.422
	1.400	1.311	1.334	1.250	1.364	1.714	1.425	1.404
me6′-1	1.452	1.297	1.292	1.258	1.359	1.728	1.406	1.422
	1.400	1.311	1.334	1.249	1.363	1.713	1.425	1.404
enol-2	1.452	1.295	1.293	1.261	1.267	1.737	1.401	1.427
	1.387	1.327	1.346	1.254	1.265	1.720	1.428	1.395

toluene, and in water and slightly distorted in the protein, especially for enol-1′ and me6′-1. This indicates that the protein environment obviously affects the geometries of the wrapped oxyluciferins and their analogues.

Absorption Spectra of the Six Chemical Forms of Oxyluciferin and Their 10 Analogues. Naumov et al.[11,17] have reported the experimental absorption spectra of oxyluciferin and oxyluciferin analogues in aqueous solution. Additionally, the subsequent estimation of pK_a* using the Förster cycle[59] requires knowing the λ_{max} values of all of the compounds. Hence, we predicted the absorption spectra for the six chemical forms of oxyluciferin and their 10 analogues in water. The predicted results are shown in Figure 4 and Table S4. Meanwhile, as we are focused on identifying the emitter, we prefer to study the emission properties. It is not necessary for us to calculate the absorption spectra in other phases besides water.

The order of the six chemical forms of oxyluciferin by theoretical calculation is consistent with that of the experimental results (Figure 4 and Tables S4 and S6). As described in Figure 4, the peaks in the absorption spectra for various types of the analogues are close to the corresponding chemical form because of a similar nature in the electronic transition (Figures S4 and S5). This indicates that the substituent groups on O10′, O11′, and C5 have little influence on the λ_{max} values. It is appropriate to study the absorption properties of the six chemical forms of oxyluciferin by their corresponding analogues experimentally.

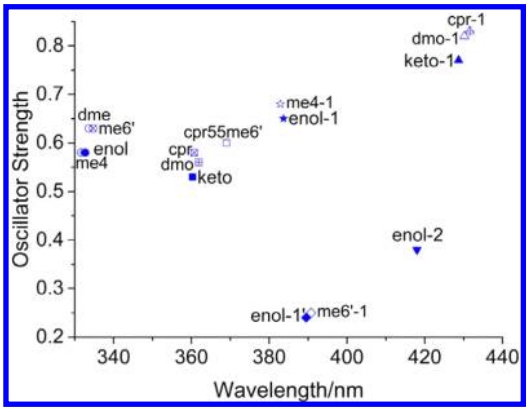

Figure 4. Oscillator strength (f) and absorption maximum (λ_{max}) of the six chemical forms of oxyluciferin and their 10 analogues in water.

Emission Spectra of the Six Chemical Forms of Oxyluciferin and Their 10 Analogues. *1. In the Gas Phase.* Although there is one experimental investigation on the absorption spectrum of oxyluciferin in the gas phase,[60] it is difficult to study the emission spectrum in the gas phase because the ion density is too low to result in enough emitted photons for detection. Theoretically, it is an easy job to predict

DOI: 10.1021/acs.jctc.5b00659
J. Chem. Theory Comput. 2015, 11, 5360−5370

λ_F and f. The calculated results for the six chemical forms of oxyluciferin and the 10 analogues in the gas phase are shown in Figure 5 and Table S5. The order of λ_F values of the six forms

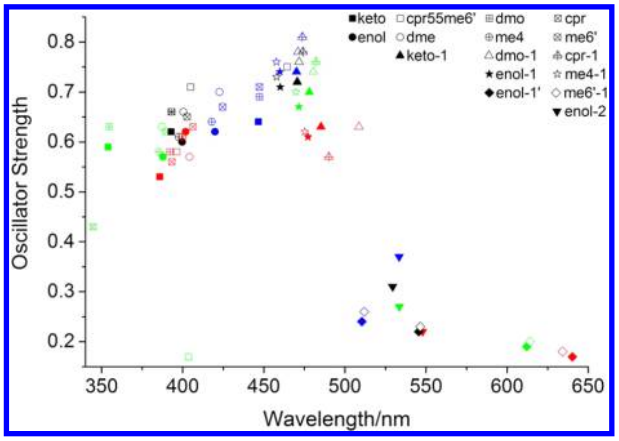

Figure 5. Fluorescence wavelength profiles of the six chemical forms of oxyluciferin and their 10 analogues in the gas phase (green), in toluene (black), in water (blue), and in a protein environment (red).

of oxyluciferin is in line with our previously calculated results using multistate complete active space second-order perturbation (MS-CASPT2).[13]

As shown in Figure 5, cpr and cpr55me6′ have a lower f than keto. These two analogues represent two major configurations in the transition (Figure S3). TD DFT is not able to address these cases reliably. This is also reflected in the optimized geometries, where the geometries of cpr and cpr55me6′ are quite different from those of keto and dmo (see details in Table S1). For the six chemical forms of oxyluciferin and their remaining eight analogues, we can see that the λ_F values of all of the ions are in the visible range (400−700 nm), whereas those of the neutral molecules are not. This suggests that the emitter exists in the ionic form. Figure 5 clearly shows that the substituents hardly affect λ_F but increase the corresponding f for each chemical form of oxyluciferin. A higher f may be obtained by the electron-donating effect of the methyl moiety. The very small red-shift tendency of analogues with O10′-methyl or C5-methyl groups is consistent with the previous conclusion.[31]

2. In Solution. The fluorescence of oxyluciferins is mostly measured in solution. We choose two solutions: water, as a simplified model for aqueous buffers, and toluene, which is similar in polarity to luciferase. In these two solutions, we theoretically predict the λ_F and f values of the S_1 states of the six chemical forms of oxyluciferin and the 10 analogues separately. The calculated results are shown in Figure 5 and Tables S4 and S5.

As described in Figure 5, the analogues have nearly the same λ_F values as their corresponding chemical form in water and toluene, except for cpr55me6′, whose λ_F values are red-shifted by 17.8 and 12 nm, respectively, compared with those of keto (detailed data are presented in Tables S4 and S5). This result occurs because cpr55me6′ has some electronic distribution on the methyl group, which differs from keto (dmo and cpr) (Figures S4−S7), and it has a large dipole moment variation from the S_0 state to the S_1 state compared with keto (dmo and cpr) (in water: keto 9.24, dmo 9.13, cpr 8.71, cpr55me6′ 9.86; in toluene: keto 7.94, dmo 7.85, cpr 7.18, cpr55me6′ 8.39). This demonstrates why cpr55me6′ emits green light and keto emits blue light in experiments.[11] In general, it is appropriate to study the λ_F values of the six chemical forms of oxyluciferin by their corresponding analogues (except for cpr55me6′) experimentally. Qualitatively, the order of the λ_F of the six chemical forms of oxyluciferin in water is partly different from that in toluene. This indicates that the solvent polarity has a significant influence on λ_F.

In toluene, only the λ_F values of the ionic forms of oxyluciferin are in the visible range. This indicates that the emitter exists in the ionic form. However, the λ_F values in water are all in the visible range because the neutral molecules display a red-shift in polar solvents.[38,61] Nevertheless, the neutral forms of oxyluciferin can be excluded as the emitter for the following reasons. First, it is generally believed that the decomposition of firefly dioxetanone starts from its anionic form,[62] which results in an ionic form of oxyluciferin in the excited state. Second, the f value of the neutral form is lower than that of the ionic form in both toluene and water such that the ionic form is necessary for high luminous efficiency. Third, the dominant fragment dissociated from oxyluciferin in firefly exists as an ion;[63] therefore, it originates from the ionic form of oxyluciferin.

The remaining four ionic forms are divided into two groups: one is keto-1 and enol-1, which have similar λ_F values and can transform by excited state keto−enol tautomerization (ESKET). The other group is enol-1′ and enol-2, which also have similar λ_F values and can transform by excited state proton transfer (ESPT). The ESKET and ESPT rates may decide the major form. Song et al.[37] deduced that keto-1 may be stabilized over enol-1 in the excited state in the protein and that a catalytic protonation path is absent, which led to the conclusion that ESKET is not likely. One year later, Solntsev et al.[32] presented the first experimental evidence of ESKET in a nonpolar and basic environment, but it is a relatively slow process. Pinto da Silva et al.[64] found that enol-based ESPT prevails over phenol-based ESPT because of the stronger hydrogen-bonding network of the enolate thiazole moiety. Ghose et al.[11] concluded that the ESPT process of enol-1′ is not likely to occur in water because the pK_a* of enol-1′/enol-2 is the largest. However, the pK_a* value of enol-1′/enol-2 is approximately 7.5, which cannot preclude the occurrence of the ESPT process in a basic solution. Moreover, the pH has a significant effect on the emission spectra because the major form of oxyluciferin changes at different pH values.[11] Thus, we cannot determine which form is the emitter from the λ_F values simply without considering the pH effect.

3. In the Protein. The above computational model that uses toluene, which has a polarity similar to that of luciferase, is too simple to identify the emitter of the natural firefly. In toluene, the neutral oxyluciferin analogues can exist in both the ground and excited states without a base or with a weak base.[20] However, in natural fireflies, the situation may be different, as there are many amino acid residues surrounding oxyluciferin that can interact, and this can influence the chemical form. Thus, it is necessary to perform calculations in the protein environment. This theoretical study is meaningful, as it is not currently easy to experimentally study the emission properties of each chemical form of oxyluciferin in vivo using oxyluciferin analogues. The QM/MM method is employed to predict the λ_F and f values of the S_1 states of the six chemical forms of oxyluciferin and the 10 analogues. The results are shown in Figure 5 and Table S5.

Qualitatively, the order of the λ_F values of the six chemical forms of oxyluciferin is the same as that in toluene. Similar to toluene, the environment surrounding the oxyluciferin is

DOI: 10.1021/acs.jctc.5b00659
J. Chem. Theory Comput. 2015, 11, 5360−5370

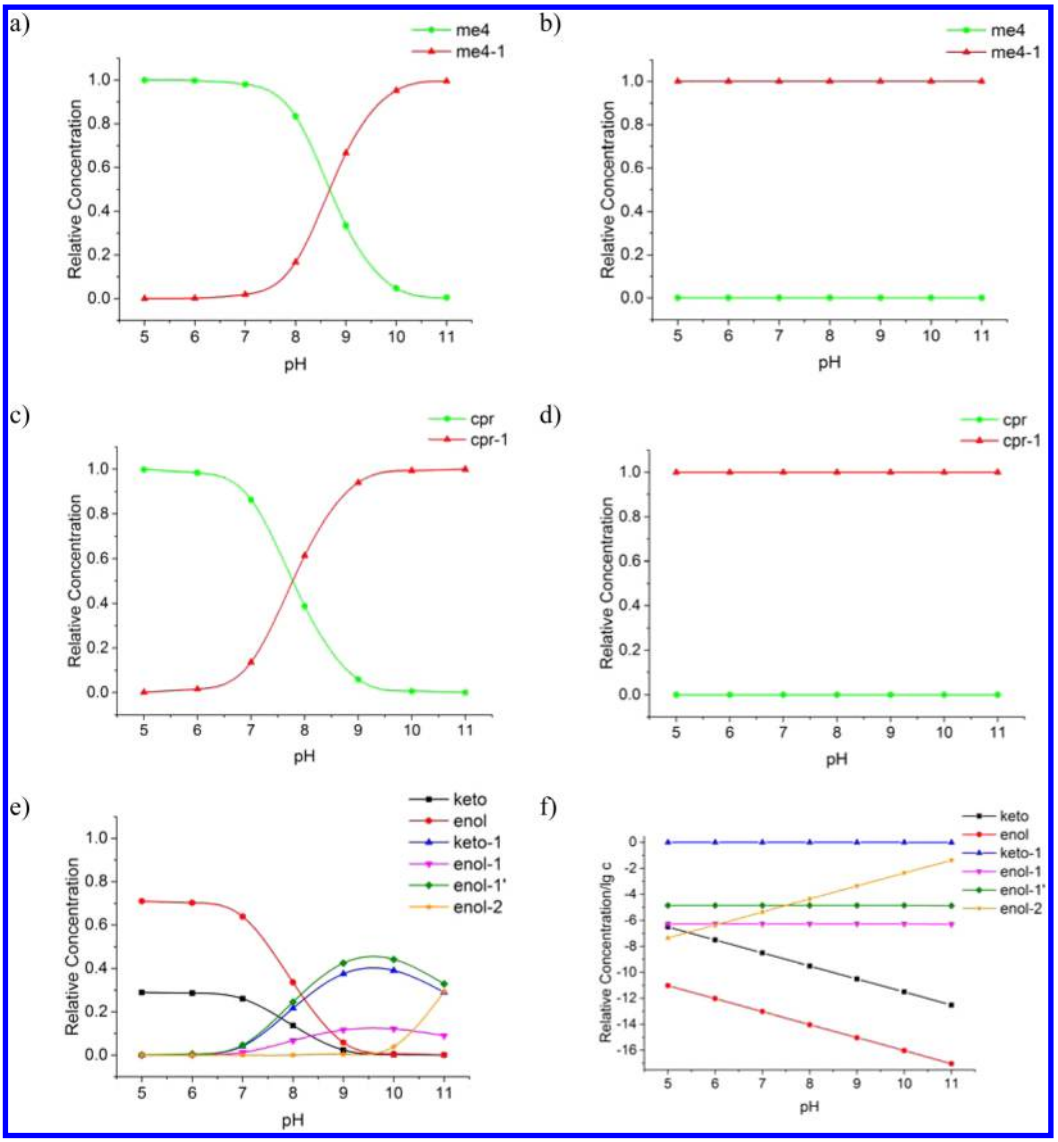

Figure 6. Calculated relative concentrations for the ground (a, c, and e) and excited (b, d, and f) states of me4, cpr, and oxyluciferin in aqueous solution at different pH (the optimum pH for the catalytic activity in vivo is ~8). The longitudinal coordinate for f is in lg c for displaying all chemical forms in one figure because the relative concentration of keto-1 is much larger than those of the other five forms.

hydrophobic and of low polarity.[18] In Figure 5, the points coordinated by the λ_F and f values of the analogues are close to those of their corresponding chemical forms. This suggests that the emission properties of the analogues studied in vivo can represent those of the corresponding chemical form of oxyluciferin.

According to Figure 5, the λ_F value of enol-1′ has a large red shift and a much lower f value compared with the other five possible emitters. Observing the electronic transition of the S_1 state of all possible emitters, only enol-1′ has a transition from the benzothiazole ring to the thiazole ring. The others all have a transition corresponding to the opposite direction (Figures S8 and S9). The structure of enol-1′ is much more distorted in the protein, but the other five possible emitters maintain a nearly planar structure in the protein. Moreover, the phenolate is necessary for the high efficiency of firefly bioluminescence.[7−9,20,65] All of these results indicate that enol-1′ is not the light emitter. The neutral forms have been excluded as discussed above; thus, one of the remaining three forms, keto-1, enol-1, or enol-2, is likely to be the emitter. To further identify the emitter from the remaining three forms, the following pH calculation and triple equilibrium analysis were carried out.

As shown in Figure 5, we can conclude the following: first, the range of λ_F for all of the chemical forms of oxyluciferin and their 10 analogues is similarly wide in the gas phase and in the protein but becomes narrow in toluene and even narrower in water; second, the f values successively increase in the protein, in the gas phase, in toluene, and in water. This indicates that the polar environment can minimize the λ_F variation among the six chemical forms of oxyluciferin and improve the luminous efficiency. The relatively wide range of λ_F in the protein is attributed to enol-1′, as its λ_F is significantly red-shifted. The λ_F range of the remaining five chemical forms in the protein is slightly narrower than that in the gas phase. This indicates that the hydrogen-bonding network can also minimize the variation in λ_F. The relative low f values in the protein may be related to CT constrained by the electrostatic interaction of the nearby amino acid residues.

The pH Influence in Aqueous Solution. The absorption and fluorescence spectra of oxyluciferin and its analogues are

DOI: 10.1021/acs.jctc.5b00659
J. Chem. Theory Comput. 2015, 11, 5360−5370

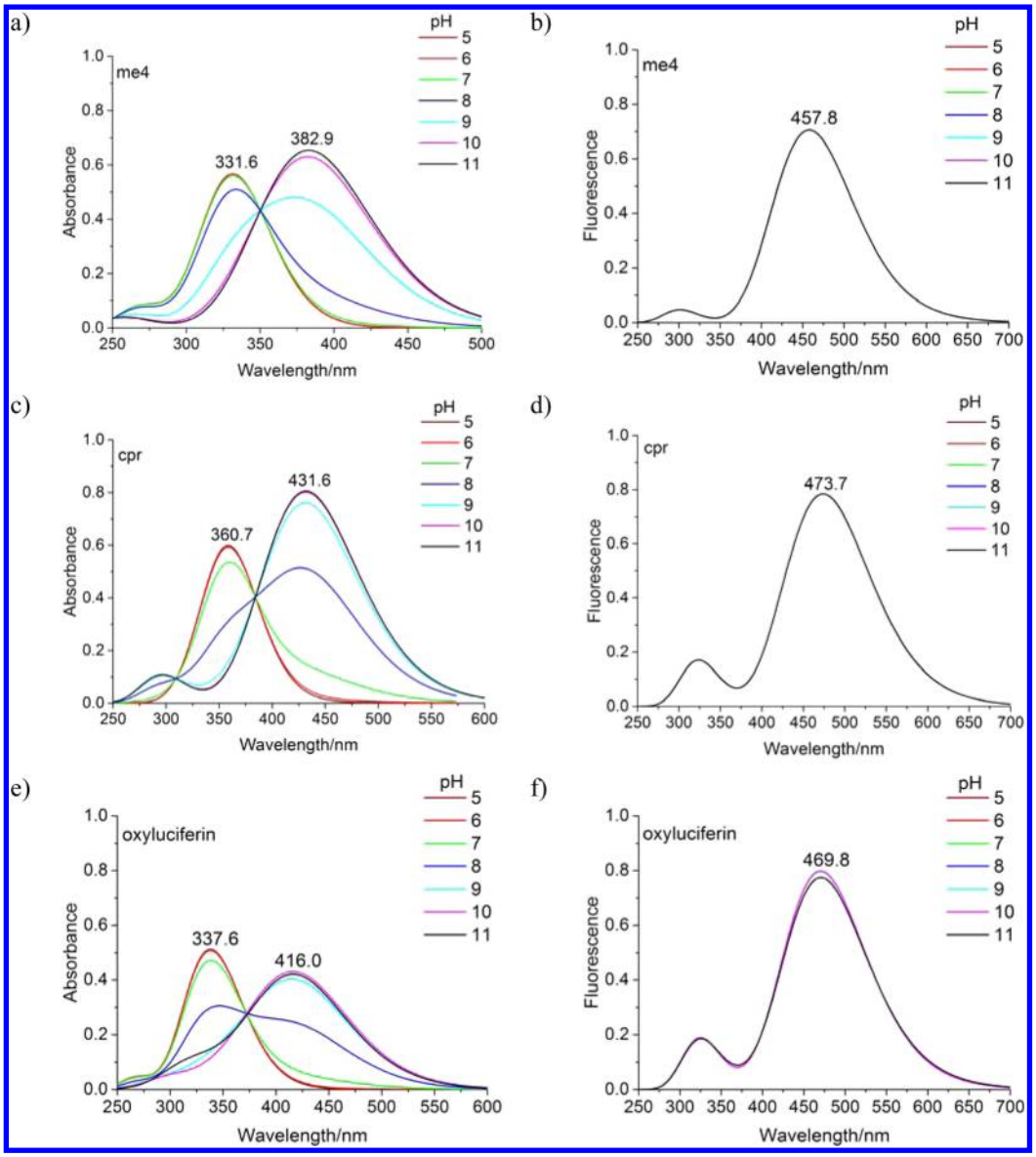

Figure 7. Fitted absorption and fluorescence spectra of me4, cpr, and oxyluciferin in aqueous solution at different pH (the optimum pH for the catalytic activity in vivo is ~8).

pH dependent.[11,17,40] Hiyama et al.[49,66−68] have reported results for the relative absorption intensities and photoluminescence of oxyluciferin and luciferin in aqueous solutions at different pH levels. On the basis of this theoretical method, we studied the dependence of the relative concentrations of different species and spectra on the pH values for both the S_0 and S_1 states of the six oxyluciferins and their analogues. Here, we select cpr, me4, cpr-1, and me4-1 as the representatives of keto, enol, keto-1, and enol-1 analogues. Three possible equilibria are considered: cpr and cpr-1; me4 and me4-1; and the mixed keto, enol, keto-1, enol-1, enol-1′, and enol-2. The diagrams of the relative concentrations and spectra with various pH values are shown in Figures 6 and 7, respectively. The details for producing Figures 6 and 7 are in the SI.

As shown in Figure 6a and c, for analogues me4 and cpr in the S_0 state, respectively, the phenol forms are the dominant species at an acidic pH. The phenolate forms become the dominant form with increasing pH. However, for both analogues in the S_1 state, the phenolate forms are the dominant species over the entire pH range (5−11) (Figure 6b and d and detail data in Table S8). This can be understood by the fact that the two analogues are photoacids.[32,69] That is, the phenolate forms cpr-1 and me4-1 should be the light emitters for the two analogues. Thus, the fitted absorption spectra show two different peaks at different pH values (Figure 7a and c), whereas the fitted fluorescence spectra have only one peak irrespective of the pH values (Figure 7b and d). The fitted absorption spectra are similar to those measured experimentally,[11] whereas the fluorescence spectra are very different. The fitted fluorescence spectra have no intensity difference at different pH values. The factors that affect fluorescence are complicated, but factors such as the concentration, nonradiative transition, and geminate proton quenching rates are all important. The currently theoretical fitting is a very rough estimate, but it is useful for drawing qualitative conclusions.

Several chemical forms of oxyluciferin may coexist at a specific pH in aqueous solution. As shown in Figure 6e, in the S_0 state, enol is the dominant species, and keto is the second

DOI: 10.1021/acs.jctc.5b00659
J. Chem. Theory Comput. 2015, 11, 5360−5370

dominant species at acidic pH values. With an increasing pH, enol-1′, keto-1, and enol-1 become the dominant species with enol-2 appearing when the pH increases to 11. Thus, the absorption spectra of oxyluciferin are formed by superposition of the spectra of several forms at specific pH values, which is consistent with experimental values[11] (Figure 7e). However, in the S_1 state, keto-1 is the dominant species over the entire pH range (5−11) (Figure 6f).[70] The calculated pK_e* value (4.5) is roughly estimated but useful in determining the direction of the change in pK_e (−0.39).[71] That is, the keto form is qualitatively more preferable in the S_1 state than in the S_0 state.[70] This explains why keto-1 is the only dominant species irrespective of the pH value. If only the concentration is considered, keto-1 is the emitter in aqueous solution. Falklöf et al.[70] also obtained the same conclusion that keto-1 is the preferred form in the S_1 state using a Born−Haber cycle calculation.

As mentioned above, the concentration factor can influence the fluorescence spectra, but it is not the only factor. The stability of the species in the S_1 state depends on the photoexcitation wavelength.[11,68] Here, a recent experimental result[11] is compared with our calculated result. When the excitation wavelength is 510 nm, the dominant species is keto-1 at pH 6−9 and changes to enol-2 at pH 10−11 based on spectral analyses.[11] As shown in Figure 6f, the same tendency can be found in our work. When the excitation wavelength is 370 nm, the dominant species is enol-1′ at an acidic pH and changes to enol-2 at a basic pH based on spectral analyses.[11] The predicted pK_a* of enol-1′/enol-2 is approximately 7.5 experimentally, which is the same as our estimation, as shown in Figure 6f. The experimental result at an excitation wavelength of 370 nm cannot conclude that keto-1 is not the emitter because when excited at 370 nm, keto-1 is shorter-lived than enol-1′ in the excited state, and the high concentration of keto-1 may be offset by the short life. Therefore, as shown in our calculated result, keto-1 is believed to be the dominant species in the excited state over a wide pH range. More importantly, this result implies that excited-state keto-1 is the main emitter at the optimum pH value (∼8) of the catalytic activity in vivo.[40,72] Quite recently, there has been strong experimental evidence that further confirms that the S_1-state keto-1 is the light emitter of the natural firefly.[10] In this experiment, the bioluminescence spectra of different luciferases tested with 6′-amino-D-luciferin almost overlap with those of its 5,5-dimethyl analogue in which enolization is blocked.[10] This result suggests that the emitted color is dependent on the polarity of the molecular environments, which agrees with the previous experimental[73] and theoretical[14,15] conclusions.

The Possible Triple Equilibrium in Protein. In 2005, Ugarova et al.[40] proposed that the firefly bioluminescence spectrum is the overlapping of the spectra of three chemical forms of oxyluciferin, i.e., keto-1 ⇆ enol-1 ⇆ enol-2. Naumov et al.[19] concluded that the above involved two chemical equilibria that can be affected by several factors, most notably pH, solvent polarity, hydrogen bonding, the presence of additional ions, and $\pi-\pi$ stacking. The effects of environmental polarity were valued via the spectral study by the same group.[20] However, these experiments were performed in vitro not in vivo. Thus, it is necessary to explore the possible triple equilibrium in a protein environment.

In our previous work, we performed the stability analysis from an energy aspect and concluded that keto-1 is the direct decomposition product of firefly dioxetanone in vivo.[13] According to the view of the triple equilibrium, keto-1 may transform into enol-1 by ESKET and into enol-2 by ESPT. According to the QM/MM optimized geometries after the MD simulation (details in the SI), in the protein, AMP, HIS247, LYS531, and one water molecule are adjacent to the oxyluciferin and may have an effect on the triple equilibrium.

ESKET involves two parts: C5 discards a proton and O11′ accepts one. According to Figure 8, the relevant bond lengths

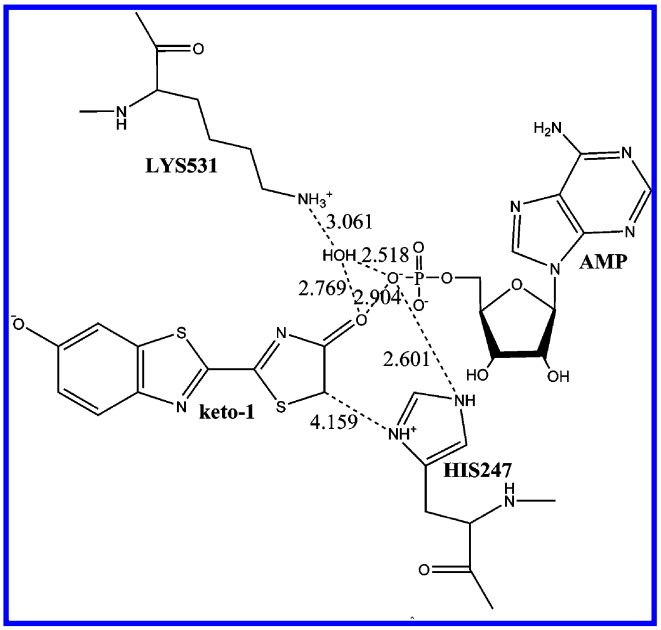

Figure 8. Two-dimensional graph for the key bond lengths (Å) of keto-1 in the protein in the excited state.

among molecules are too long, and it is not easy to form effective hydrogen bonding interactions. On the basis of this hydrogen bond analysis, a reaction path for ESKET is lacking. Song et al.[37] reported the same conclusion. In terms of the thermal stability, a slight issue exists regarding whether ESKET from keto-1 to enol-1 in the protein is feasible[13] or not.[37] No matter which of the two (keto-1 and enol-1) is more stable in the S_1 state, formation of a hydrogen bond surrounding O11′ and C5 of keto-1 is not likely. Thus, ESKET is not likely, and subsequently, ESPT could not occur. Moreover, in real lives, the pH value and microenvironment are fixed. On the basis of in vivo studies on the emission spectra of 35 species of fireflies,[74,75] Seliger's group concluded that "the emission is most likely due to a single excited enzyme-substrate complex".[76] Therefore, keto-1 is the main emitter.

CONCLUSIONS

The identification of the light emitter of fireflies has been explored for many years. The problem is still being debated, although a consistent conclusion was almost reached in 2011. To solve the debate, we computed spectra for all six chemical forms of oxyluciferin and their corresponding analogues in the gas phase, in toluene, and in water using TD DFT and compared the results with the latest experimental data. The impact of the real protein environment was also investigated using QM/MM combined with MD. CAM-B3LYP was employed because it has long-range corrections and performs well for the description of CT excited states. During the bioluminescence process of a firefly, the evidence of the dioxetanone decomposing from its anionic form, the λ_F apart

DOI: 10.1021/acs.jctc.5b00659
J. Chem. Theory Comput. 2015, 11, 5360−5370

from the visible light and the relatively low *f* values, and the fact that oxyluciferin dissociates into anionic fragments, keto, enol, and enol-1′ were excluded as the light emitters. Subsequently, the pH effect was calculated and discussed. On the basis of the obtained relative concentrations of all six chemical forms in the excited state and combined with the optimum pH for the catalytic activity in vivo, keto-1 is believed to be the main emitter. The triple equilibrium was also explored in the protein. This equilibrium is not likely to occur based on the hydrogen-bond analysis and considering a fixed microenvironment in real lives; thus, keto-1 is still the main emitter. Additionally, the calculation of the analogues indicates that the emission properties of the analogues can represent those of the corresponding chemical form of oxyluciferin in general, and these calculations in the protein provide information to supplement experimental research.

■ ASSOCIATED CONTENT

Supporting Information

The Supporting Information is available free of charge on the ACS Publications website at DOI: 10.1021/acs.jctc.5b00659.

Computational details; details of the pH-dependent spectra calculation; key geometric parameters of all of the compounds in different phases; detailed data for wavelength and relative concentration; frontier molecular orbital plots of all of the compounds in different phases; superposition of different chemical forms; superposition of oxyluciferin and its corresponding analogues; Cartesian coordinates of all of the optimized equilibrium structures (PDF)

■ AUTHOR INFORMATION

Corresponding Author

*E-mail: yajun.liu@bnu.edu.cn.

Notes

The authors declare no competing financial interest.

■ ACKNOWLEDGMENTS

The authors appreciate Prof. Nicolas Ferré for his help to combine the Gaussian and Tinker codes. This work was supported by grants from the National Natural Science Foundation of China (Grants 21273021, 21325312, and 21421003) and the Major State Basic Research Development Programs (Grant 2011CB808500).

■ REFERENCES

(1) Ando, Y.; Niwa, K.; Yamada, N.; Enomoto, T.; Irie, T.; Kubota, H.; Ohmiya, Y.; Akiyama, H. *Nat. Photonics* **2008**, *2*, 44−47.

(2) Dothager, R. S.; Flentie, K.; Moss, B.; Pan, M.-H.; Kesarwala, A.; Piwnica-Worms, D. *Curr. Opin. Biotechnol.* **2009**, *20*, 45−53.

(3) Michelini, E.; Cevenini, L.; Calabretta, M. M.; Calabria, D.; Roda, A. *Anal. Bioanal. Chem.* **2014**, *406*, 5531−5539.

(4) Zhang, Y. M.; Wang, X. J.; Li, W.; Zhang, W. R.; Li, M. J.; Zhang, S. X. A. *Chem. Commun.* **2014**, *50*, 13477−13480.

(5) Fraga, H. *Photochem. Photobiol. Sci.* **2008**, *7*, 146−158.

(6) McElroy, W. D.; Seliger, H. H.; White, E. H. *Photochem. Photobiol.* **1969**, *10*, 153−170.

(7) Yue, L.; Liu, Y.-J.; Fang, W.-H. *J. Am. Chem. Soc.* **2012**, *134*, 11632−11639.

(8) Liu, F. Y.; Liu, Y. J.; De Vico, L.; Lindh, R. *J. Am. Chem. Soc.* **2009**, *131*, 6181−6188.

(9) Liu, F. Y.; Liu, Y. J.; De Vico, L.; Lindh, R. *Chem. Phys. Lett.* **2009**, *484*, 69−75.

(10) Viviani, V. R.; Neves, D. R.; Amaral, D. T.; Prado, R. A.; Matsuhashi, T.; Hirano, T. *Biochemistry* **2014**, *53*, 5208−5220.

(11) Ghose, A.; Rebarz, M.; Maltsev, O. V.; Hintermann, L.; Ruckebusch, C.; Fron, E.; Hofkens, J.; Mély, Y.; Naumov, P.; Sliwa, M.; Didier, P. *J. Phys. Chem. B* **2015**, *119*, 2638−2649.

(12) Branchini, B. R.; Murtiashaw, M. H.; Magyar, R. A.; Portier, N. C.; Ruggiero, M. C.; Stroh, J. G. *J. Am. Chem. Soc.* **2002**, *124*, 2112−2113.

(13) Chen, S.-F.; Liu, Y.-J.; Navizet, I.; Ferré, N.; Fang, W.-H.; Lindh, R. *J. Chem. Theory Comput.* **2011**, *7*, 798−803.

(14) Navizet, I.; Liu, Y.-J.; Ferré, N.; Xiao, H.-Y.; Fang, W.-H.; Lindh, R. *J. Am. Chem. Soc.* **2010**, *132*, 706−712.

(15) Liu, Y.-J.; De Vico, L.; Lindh, R. *J. Photochem. Photobiol., A* **2008**, *194*, 261−267.

(16) Maltsev, O. V.; Nath, N. K.; Naumov, P.; Hintermann, L. *Angew. Chem., Int. Ed.* **2014**, *53*, 847−850.

(17) Rebarz, M.; Kukovec, B.-M.; Maltsev, O. V.; Ruckebusch, C.; Hintermann, L.; Naumov, P.; Sliwa, M. *Chem. Sci.* **2013**, *4*, 3803−3809.

(18) Hirano, T.; Hasumi, Y.; Ohtsuka, K.; Maki, S.; Niwa, H.; Yamaji, M.; Hashizume, D. *J. Am. Chem. Soc.* **2009**, *131*, 2385−2396.

(19) Naumov, P.; Ozawa, Y.; Ohkubo, K.; Fukuzumi, S. *J. Am. Chem. Soc.* **2009**, *131*, 11590−11605.

(20) Naumov, P.; Kochunnoonny, M. *J. Am. Chem. Soc.* **2010**, *132*, 11566−11579.

(21) Ugarova, N. N. *Photochem. Photobiol. Sci.* **2008**, *7*, 218−227.

(22) Wood, K. V. *Photochem. Photobiol.* **1995**, *62*, 662−673.

(23) Viviani, V. R. *Cell. Mol. Life Sci.* **2002**, *59*, 1833−1850.

(24) White, E. H.; Rapaport, E.; Seliger, H. H.; Hopkins, T. A. *Bioorg. Chem.* **1971**, *1*, 92−122.

(25) McCapra, F.; Gilfoyle, D. J.; Young, D. W.; Church, N. J.; Spencer, P. In *Bioluminescence and Chemiluminescence*; Campbell, A. K., Kricka, L. J., Stanley, P. E., Eds.; John Wiley & Sons: Chichester, 1994; p 387.

(26) Orlova, G.; Goddard, J. D.; Brovko, L. Y. *J. Am. Chem. Soc.* **2003**, *125*, 6962−6971.

(27) Yang, T. X.; Goddard, J. D. *J. Phys. Chem. A* **2007**, *111*, 4489−4497.

(28) Nakatani, N.; Hasegawa, J.-y.; Nakatsuji, H. *J. Am. Chem. Soc.* **2007**, *129*, 8756−8765.

(29) Branchini, B. R.; Southworth, T. L.; Murtiashaw, M. H.; Magyar, R. A.; Gonzalez, S. A.; Ruggiero, M. C.; Stroh, J. G. *Biochemistry* **2004**, *43*, 7255−7262.

(30) Nakatsu, T.; Ichiyama, S.; Hiratake, J.; Saldanha, A.; Kobashi, N.; Sakata, K.; Kato, H. *Nature* **2006**, *440*, 372−376.

(31) Ran, X. Q.; Zhou, X.; Goddard, J. D. *ChemPhysChem* **2015**, *16*, 396−402.

(32) Solntsev, K. M.; Laptenok, S. P.; Naumov, P. *J. Am. Chem. Soc.* **2012**, *134*, 16452−16455.

(33) Ren, A.-M.; Guo, J.-F.; Feng, J.-F.; Zou, L.-Y.; Li, Z.-W.; Goddard, J. D. *Chin. J. Chem.* **2008**, *26*, 55−64.

(34) Pinto da Silva, L.; Simkovitch, R.; Huppert, D.; Esteves da Silva, J. C. G. *ChemPhysChem* **2013**, *14*, 3441−3446.

(35) da Silva, L. P.; Esteves da Silva, J. C. G. *J. Chem. Theory Comput.* **2011**, *7*, 809−817.

(36) Sakai, H.; Wada, N. *Comput. Theor. Chem.* **2014**, *1045*, 93−98.

(37) Song, C.-i.; Rhee, Y. M. *J. Am. Chem. Soc.* **2011**, *133*, 12040−12049.

(38) Pinto da Silva, L.; Esteves da Silva, J. C. G. *ChemPhysChem* **2011**, *12*, 951−960.

(39) Pinto da Silva, L.; Esteves da Silva, J. C. G. *J. Phys. Chem. B* **2015**, *119*, 2140−2148.

(40) Ugarova, N. N.; Maloshenok, L. G.; Uporov, I. V.; Koksharov, M. I. *Biochemistry* **2005**, *70*, 1262−1267.

(41) Perdew, J. P.; Ruzsinszky, A.; Tao, J. M.; Staroverov, V. N.; Scuseria, G. E.; Csonka, G. I. *J. Chem. Phys.* **2005**, *123*, 062201−062209.

(42) Dreuw, A.; Head-Gordon, M. *Chem. Rev.* **2005**, *105*, 4009−4037.

DOI: 10.1021/acs.jctc.5b00659
J. Chem. Theory Comput. 2015, 11, 5360−5370

(43) Stratmann, R. E.; Scuseria, G. E.; Frisch, M. J. *J. Chem. Phys.* **1998**, *109*, 8218−8224.
(44) Runge, E.; Gross, E. K. U. *Phys. Rev. Lett.* **1984**, *52*, 997−1000.
(45) Yanai, T.; Tew, D. P.; Handy, N. C. *Chem. Phys. Lett.* **2004**, *393*, 51−57.
(46) Becke, A. D. *Phys. Rev. A: At., Mol., Opt. Phys.* **1988**, *38*, 3098−3100.
(47) Lee, C. T.; Yang, W. T.; Parr, R. G. *Phys. Rev. B: Condens. Matter Mater. Phys.* **1988**, *37*, 785−789.
(48) Cheng, Y.-Y.; Zhu, J.; Liu, Y.-J. *Chem. Phys. Lett.* **2014**, *591*, 156−160.
(49) Hiyama, M.; Akiyama, H.; Wang, Y.; Koga, N. *Chem. Phys. Lett.* **2013**, *577*, 121−126.
(50) Barone, V.; Cossi, M. *J. Phys. Chem. A* **1998**, *102*, 1995−2001.
(51) Cossi, M.; Rega, N.; Scalmani, G.; Barone, V. *J. Chem. Phys.* **2001**, *114*, 5691−5701.
(52) Cossi, M.; Rega, N.; Scalmani, G.; Barone, V. *J. Comput. Chem.* **2003**, *24*, 669−681.
(53) Frisch, M. J.; Trucks, G. W.; Schlegel, H. B.; Scuseria, G. E.; Robb, M. A.; Cheeseman, J. R.; Scalmani, G.; Barone, V.; Mennucci, B.; Petersson, G. A.; Nakatsuji, H.; Caricato, M.; Li, X.; Hratchian, H. P.; Izmaylov, A. F.; Bloino, J.; Zheng, G.; Sonnenberg, J. L.; Hada, M.; Ehara, M.; Toyota, K.; Fukuda, R.; Hasegawa, J.; Ishida, M.; Nakajima, T.; Honda, Y.; Kitao, O.; Nakai, H.; Vreven, T.; Montgomery, J. A., Jr.; Peralta, J. E.; Ogliaro, F.; Bearpark, M.; Heyd, J. J.; Brothers, E.; Kudin, K. N.; Staroverov, V. N.; Kobayashi, R.; Normand, J.; Raghavachari, K.; Rendell, A.; Burant, J. C.; Iyengar, S. S.; Tomasi, J.; Cossi, M.; Rega, N.; Millam, J. M.; Klene, M.; Knox, J. E.; Cross, J. B.; Bakken, V.; Adamo, C.; Jaramillo, J.; Gomperts, R.; Stratmann, R. E.; Yazyev, O.; Austin, A. J.; Cammi, R.; Pomelli, C.; Ochterski, J. W.; Martin, R. L.; Morokuma, K.; Zakrzewski, V. G.; Voth, G. A.; Salvador, P.; Dannenberg, J. J.; Dapprich, S.; Daniels, A. D.; Farkas, O.; Foresman, J. B.; Ortiz, J. V.; Cioslowski, J.; Fox, D. J. *Gaussian 09*, revision A.02; Gaussian, Inc.: Wallingford, CT, 2009.
(54) Ponder, J. W. *TINKER, Software Tools for Molecular Design*, version 4.2; Department of Biochemistry and Molecular Biophysics, Washington University School of Medicine: St. Louis, MO, 2004. The most updated version for the TINKER program can be obtained from the Internet at http://dasher.wustl.edu/tinker.
(55) Zhou, J.-G.; Williams, Q. L.; Walters, W., Jr.; Deng, Z.-Y. *J. Phys. Chem. B* **2015**, *119*, 10399−10405.
(56) Ferré, N.; Ángyán, J. G. *Chem. Phys. Lett.* **2002**, *356*, 331−339.
(57) Hornak, V.; Abel, R.; Okur, A.; Strockbine, B.; Roitberg, A.; Simmerling, C. *Proteins: Struct., Funct., Genet.* **2006**, *65*, 712−725.
(58) Case, D. A.; Darden, T. A.; Cheatham, T. E., III; Simmerling, C. L.; Wang, J.; Duke, R. E.; Luo, R.; Merz, K. M.; Pearlman, D. A.; Crowley, M.; Walker, R. C.; Zhang, W.; Wang, B.; Hayik, S.; Roitberg, A.; Seabra, G.; Wong, K. F.; Paesani, F.; Wu, X.; Brozell, S.; Tsui, V.; Gohlke, H.; Yang, L.; Tan, C.; Mongan, J.; Hornak, V.; Cui, G.; Beroza, P.; Mathews, D. H.; Schafmeister, C.; Ross, W. S.; Kollman, P. A. *AMBER 9*; University of California: San Francisco, CA, 2006.
(59) Lakowicz, J. R. In *Principles of Fluorescence Spectroscopy*, 3rd ed.; Springer: New York, 2006; p 259.
(60) Støchkel, K.; Hansen, C. N.; Houmøller, J.; Nielsen, L. M.; Anggara, K.; Linares, M.; Norman, P.; Nogueira, F.; Maltsev, O. V.; Hintermann, L.; Nielsen, S. B.; Naumov, P.; Milne, B. F. *J. Am. Chem. Soc.* **2013**, *135*, 6485−6493.
(61) da Silva, L. P.; Esteves da Silva, J. C. G. *J. Comput. Chem.* **2011**, *32*, 2654−2663.
(62) Shimomura, O. In *Bioluminescence Chemical Principles and Methods*; World Scientific Publishing Co. Pte. Ltd.: Singapore, 2006; p 1.
(63) Jensen, M. W.; Støchkel, K.; Kjær, C.; Knudsen, J. L.; Maltsev, O. V.; Hintermann, L.; Naumov, P.; Milne, B. F.; Nielsen, S. B. *Int. J. Mass Spectrom.* **2014**, *365*, 3−9.
(64) Pinto da Silva, L.; Esteves da Silva, J. C. G. *ChemPhysChem* **2015**, *16*, 455−464.
(65) Chung, L. W.; Hayashi, S.; Lundberg, M.; Nakatsu, T.; Kato, H.; Morokuma, K. *J. Am. Chem. Soc.* **2008**, *130*, 12880−12881.
(66) Hiyama, M.; Akiyama, H.; Yamada, K.; Koga, N. *Photochem. Photobiol.* **2013**, *89*, 571−578.
(67) Hiyama, M.; Akiyama, H.; Yamada, K.; Koga, N. *Photochem. Photobiol.* **2014**, *90*, 35−44.
(68) Hiyama, M.; Mochizuki, T.; Akiyama, H.; Koga, N. *Photochem. Photobiol.* **2015**, *91*, 74−83.
(69) Erez, Y.; Presiado, I.; Gepshtein, R.; Pinto da Silva, L.; Esteves da Silva, J. C. G.; Huppert, D. *J. Phys. Chem. A* **2012**, *116*, 7452−7461.
(70) Falklöf, O.; Durbeej, B. *J. Comput. Chem.* **2014**, *35*, 2184−2194.
(71) Lakowicz, J. R. In *Principles of Fluorescence Spectroscopy*; 3rd ed.; Springer: New York, 2006; p 262.
(72) Woodroofe, C. C.; Meisenheimer, P. L.; Klaubert, D. H.; Kovic, Y.; Rosenberg, J. C.; Behney, C. E.; Southworth, T. L.; Branchini, B. R. *Biochemistry* **2012**, *51*, 9807−9813.
(73) Hirano, T.; Nagai, H.; Matsuhashi, T.; Hasumi, Y.; Iwano, S.; Ito, K.; Maki, S.; Niwa, H.; Viviani, V. R. *Photochem. Photobiol. Sci.* **2012**, *11*, 1281−1284.
(74) Seliger, H. H.; Buck, J. B.; Fastie, W. G.; McElroy, W. D. *J. Gen. Physiol.* **1964**, *48*, 95−104.
(75) Biggley, W. H.; Lloyd, J. E.; Seliger, H. H. *J. Gen. Physiol.* **1967**, *50*, 1681−1692.
(76) Seliger, H. H.; McElroy, W. D. *Proc. Natl. Acad. Sci. U. S. A.* **1964**, *52*, 75−81.

DOI: 10.1021/acs.jctc.5b00659
J. Chem. Theory Comput. 2015, 11, 5360−5370